ISSN 1330–0016
CODEN FIZBE7

ELECTROPRODUCTION OF HADRONS ON NUCLEI AT GeV ENERGIES

TH. FALTER[1] and U. MOSEL

Institut für Theoretische Physik, Universität Giessen, D-35392 Giessen, Germany
[1]*E-mail address: Thomas.Falter@theo.physik.uni-giessen.de*

Received 27 August 2003; Accepted 26 April 2004
Online 10 October 2004

We investigate coherence-length effects and hadron attenuation in lepton scattering off nuclei in the kinematic regime of the HERMES experiment. The elementary electron-nucleon interaction is described within the event generator PYTHIA, while a full coupled-channel treatment of the final-state interactions is included by means of a BUU transport model. The results of our calculations are in good agreement with the experimentally measured transparency ratio of incoherent ρ^0 electroproduction off ^{14}N and the multiplicity ratio $R_{\mathrm{M}}^{\mathrm{h}}$ for charged hadrons, pions, kaons, protons and anti-protons in deep inelastic scattering off ^{14}N and ^{84}Kr targets.

PACS numbers: 25.20.Dc, 24.10.Ht, 12.40.Vv UDC 539.12
Keywords: deep inelastic scattering, meson electroproduction, Glauber theory, BUU transport model

1. Introduction

High-energy meson electroproduction off complex nuclei offers a promising tool to study the physics of hadron formation. The relatively clean nuclear environment of electron-induced reactions makes it possible to investigate the timescale of the hadronization process as well as the properties of hadrons immediately after their creation. In addition, one can vary the energy and virtuality of the exchanged photon to examine the phenomenon of colour transparency [1].

In previous works [2 − 4] we have developed a method to combine the quantum mechanical coherence in the entrance channel of photonuclear reactions with a full coupled-channel treatment of the final-state interactions (FSI) in the framework of a semi-classical transport model. This allows us to include a much broader class of final-state interactions than usual Glauber theory.

In Refs. [2] and [3], we have shown that side-feeding effects that are absent in calculations based on Glauber theory might play an important role in semi-inclusive photoproduction experiments. In Ref. [4], we have then investigated the transparency ratio of exclusive incoherent ρ^0 electroproduction off ^{14}N and ^{84}Kr within our model and found excellent agreement with the nitrogen data [5] from the HERMES collaboration. The most important elementary process for this reaction was found to be diffractive ρ^0 production on bound nucleons. Other production mechanisms were supressed by the stringent exclusivity measure imposed by experiment. We found no signature for colour transparency in the data for the transparency ratio

$$T_A = \frac{\sigma_{\gamma^* \mathrm{A} \to \rho^0 \mathrm{A}^*}}{A \sigma_{\gamma^* \mathrm{N} \to \rho^0 \mathrm{N}}} \tag{1}$$

as a function of the ρ^0 coherence length, meaning that in our model calculations we could assume that the diffractively produced ρ^0 starts to interact with a hadronic cross section right after its production. However, Kopeliovich et al. [6] have pointed out that the missing signal of colour transparency might be an accidental consequence of the specific correlation between the Q^2 of the photon and the coherence length of the ρ^0 in the HERMES data.

A finite formation time of hadrons becomes visible in our investigation [7] of the HERMES data on charged particle multiplicities in deep inelastic lepton scattering (DIS) off nuclei [8, 9]. In the DIS regime, we assume that the primary production mechanism is governed by the excitation and decay of a hadronic string. The fragmentation of the string and the hadronization of the fragments takes some time (formation time τ_f). After their formation time, the reaction products undergo hadronic final-state interactions with nucleons in the target nucleus. Due to time dilatation the formation time, t_f in the target rest frame can become quite large

$$t_\mathrm{f} = \gamma \cdot \tau_\mathrm{f} = \frac{z_\mathrm{h} \nu}{m_\mathrm{h}} \tau_\mathrm{f}. \tag{2}$$

Here m_h denotes the hadron mass and z_h is the fraction of the photon energy ν that is carried away by the hadron. For high energies and for very light fragments, e.g. pions, the formation length can easily exceed the size of a nucleus. This, however, is not the case for the heavier fragments such as baryons and vector mesons for which the formation length at HERMES energies is still of the order of the nuclear radius so that “classical” nuclear interactions must play a role for these particles. In our, model the prehadronic interactions of the constituent quarks from the string ends during the formation time are effectively accounted for by using the concept of leading hadrons which is in accordance with other transport models for high energy reactions such as the UrQMD [10] and the HSD model [11, 12]. Alternative explanations for the observed modification of the multiplicity spectra in terms of a possible rescaling of the fragmentation function in nuclei [13] or a purely partonic energy loss [14, 15] through multiple scattering of the struck quark and induced gluon bremsstrahlung may model these prehadronic interactions, but may neglect the classical FSI after formation.

The formation time also plays an important role in studies of ultrarelativistic heavy ion reactions. For example, the observed quenching of high transverse momentum hadrons in $\mathrm{Au} + \mathrm{Au}$ reactions relative to $\mathrm{p} + \mathrm{p}$ collisions is often thought to be due to jet quenching in a quark gluon plasma. However, the attenuation of high p_T hadrons might also be due to hadronic rescattering processes [16] if the hadron formation time τ_f (in its rest frame) is sufficiently short.

Our paper is structured in the following way: In Sect. 2.1 we show how we describe the electron-nucleon interaction and how we account for shadowing within our model. The transport model is sketched in Sect. 2.2. Our result for the transparency ratio of incoherent ρ^0 electroproduction is presented in Sect. 3.1 in comparison with experimental data from the HERMES experiment. In Sect. 3.2 we show the calculated multiplicity ratio for charged hadrons, pions, kaons, protons and anti-protons. We close with a short summary in Sect. 4.

2. Model

In our approach the lepton-nucleus interaction is splitted into two parts: 1) In the first step, the virtual photon is absorbed on a bound nucleon of the target; this interaction produces a bunch of particles that in step 2) are propagated within the transport model. Coherence length effects in the entrance channel, that give rise to nuclear shadowing, are taken into account as described in Ref. [3].

2.1. Elementary photon nucleon interaction and shadowing

We use the event generator PYTHIA v6.2 [17] to describe the interaction of the virtual photon and a nucleon. The basic idea is that in a photon-hadron collision the physical photon γ not necessarily interacts as a point particle γ_0 (direct interaction) but might fluctuate into a vector meson V$= \rho^0, \omega, \phi, \mathrm{J}/\Psi$ (vector meson dominance, VMD) or perturbatively branch into a $q\bar{q}$ pair before the interaction (generalized vector meson dominance, GVMD). We have shown in Ref. [4] that the latter is very unlikely in the kinematic regime of the HERMES experiment (photon energy $\nu \approx 7 - 23.4$ GeV, $Q^2 \approx 0.5 - 5$ GeV^2). In most cases, the photon will therefore interact directly with a parton of the target nucleon (DIS) or fluctuate into a vector meson (VMD) before it reaches the nucleon. In the latter case, the vector meson might either scatter diffractively from the nucleon or a hard scattering between the constituents of the vector meson and the nucleon might take place. The hard scattering like the direct photon–nucleon interaction leads to the excitation of one or more hadronic strings which finally fragment into hadrons.

If the struck nucleon is embedded in a nucleus, one has to account for its Fermi motion and binding energy as well as for Pauli blocking of final-state nucleons. In addition, one has to be aware that the nuclear environment influences the VMD part of the photon-nucleon interaction, since the vector meson components get modified on their way through the nuclear medium to the interaction point. The latter has been investigated in detail in Ref. [4]. There we have shown that at the position $\boldsymbol{r}$ inside the nucleus, the physical photon state has changed to

$$|\gamma(\boldsymbol{r})\rangle = \left(1 - \sum_{\mathrm{V}=\rho,\omega,\phi,\mathrm{J}/\Psi} \frac{e^2}{2g_\mathrm{V}^2} F_\mathrm{V}^2\right) |\gamma_0\rangle + \sum_{\mathrm{V}=\rho,\omega,\phi,\mathrm{J}/\Psi} \frac{e}{g_\mathrm{V}} F_\mathrm{V} \left(1 - \overline{\Gamma_\mathrm{V}^{(\mathrm{A})}}(\boldsymbol{r})\right) |V\rangle \quad (3)$$

due to these 'initial state interactions' of the photon. The formfactor F_V from Ref. [18] accounts also for contributions of longitudinal photons. If one neglects any influence of the FSI for the moment, the reaction amplitude for the process γN →f on a nucleon at position $\boldsymbol{r}$ inside a nucleus changes compared to the vacuum in the following way

$$\langle f|\hat{T}|\gamma\rangle \to \langle f|\hat{T}|\gamma(\boldsymbol{r})\rangle. \quad (4)$$

The nuclear profile function $\Gamma_\mathrm{V}^{(\mathrm{A})}(\boldsymbol{r})$ can be expressed as

$$\begin{aligned}\overline{\Gamma_\mathrm{V}^{(\mathrm{A})}}(\boldsymbol{b},z) &= \int_{-\infty}^{z} \mathrm{d}z_i n(\boldsymbol{b},z_i)(1-j_0(q_c|z_i-z|))\frac{\sigma_\mathrm{VN}}{2}(1-\mathrm{i}\alpha_\mathrm{V})\mathrm{e}^{\mathrm{i}q_\mathrm{V}(z_i-z)} \\ &\quad \times \exp\left[-\frac{1}{2}\sigma_\mathrm{VN}(1-\mathrm{i}\alpha_\mathrm{V})\int_{z_i}^{z}\mathrm{d}z_k n(\boldsymbol{b},z_k)\right] \quad (5)\end{aligned}$$

with the nucleon number density $n(\boldsymbol{r})$, the total vector meson nucleon cross section σ_VN and the ratio α_V of real to imaginary part of the vector meson nucleon forward scattering amplitude. The Bessel function parametrization with $q_c = 0.78$ GeV avoids unphysical contributions from processes where $z_i \approx z$ which would contribute for small values of the coherence length l_V. In Ref. [19], we have shown that this Bessel function parameterization yields a good description of shadowing in photoabsorption down to the onset region of shadowing.

The probability that the photon interacts with a bound nucleon via a certain vector meson fluctuation therefore depends on the position inside the nucleus. The momentum transfer

$$q_\mathrm{V} = \sqrt{\nu^2 + Q^2} - \sqrt{\nu^2 - m_\mathrm{V}^2} \quad (6)$$

in the phase factor of Eq. (5) equals the inverse of the coherence length l_V of a vector meson component V, i.e. the length that the photon travels as a vector meson fluctuation estimated via the uncertainty principle.

2.2. Transport model

The propagation of the produced final state $|f\rangle$ through the nucleus is treated within a semi-classical transport model based on the Boltzmann-Uehling-Uhlenbeck (BUU) equation. The BUU equation describes the time evolution of the phase space density $f_i(\boldsymbol{r},\boldsymbol{p},t)$ of particles of type i that can interact via binary reactions. Besides the nucleons, these particles involve baryonic resonances and mesons (π, η, ρ, K, ...)

that are produced either in the primary reaction or during the FSI. For a particle species i the BUU equation can be written as

$$\left(\frac{\partial}{\partial t}+\frac{\partial H}{\partial \boldsymbol{p}}\frac{\partial}{\partial \boldsymbol{r}}-\frac{\partial H}{\partial \boldsymbol{r}}\frac{\partial}{\partial \boldsymbol{p}}\right)f_i(\boldsymbol{r},\boldsymbol{p},t)=I_{\mathrm{coll}}[f_1,...f_i,...,f_M]. \tag{7}$$

For baryons, the Hamilton function H includes a mean field potential which depends on the particle position and momentum. The collision integral on the right hand side accounts for the creation and annihilation of particles of type i in a collision as well as elastic scattering from one position in phase space into another. For fermions, Pauli blocking is taken into account in I_{coll} via blocking factors. The BUU equations of each particle species i are coupled via the mean field and the collision integral. The resulting system of coupled differential-integral equations is solved via a test particle ansatz for the phase space density. We also stress that within our model unstable particles might decay during their propagation through the nucleus. For details of the transport model see Ref. [20].

The classes of FSI that are included in the transport model go far beyond what can be achieved within the Glauber theory. As a result, the finally observed particles do not need to be created in the primary reaction, but might be produced during the FSI via side feeding. It is therefore clear that a purely absorptive treatment of the FSI as in Glauber theory can only be used if one is sure that one has eliminated the possibility of side feeding by applying enough constraints on the observable (see Ref. [3] for details). This might be possible for exclusive ρ^0 production measured at HERMES, but becomes questionable for the measurement of inclusive hadron multiplicity spectra.

As discussed in Sect. 2.1, a hard primary photon–nucleon interaction leads to the excitation of hadronic strings. The time, that is needed for the fragmentation of the strings and for the hadronization of the fragments, we denote as formation time τ_{f} in line with the convention in transport models. For simplicity, we assume that the formation time is a constant τ_{f} in the rest frame of each hadron and that it does not depend on the particle species. In principle, one expects a distribution in the formation times, however, and we here address only the mean value of such an 'unknown' distribution. We recall that due to time dilatation, the formation time t_{f} in the laboratory frame is then proportional to the particle energy as can be seen from Eq. (2). The size of τ_{f} can be estimated by the time that the constituents of the hadrons need to travel a distance of a typical hadronic radius ($0.5-0.8$ fm). We assume that hadrons, whose constituent quarks and antiquarks are created from the vacuum in the string fragmentation, do not interact with the surrounding nuclear medium within their formation time. For the leading hadrons, i.e. those involving quarks (antiquarks) from the struck nucleon or the hadronic components of the photon, we assume a reduced effective cross section σ_{lead} during the formation time τ_{f} and the full hadronic cross section σ_{h} [21] later on. This concept is illustrated in Fig. 1; due to the time dilatation, light particles emerging from the middle of the string might escape the nucleus without further interaction if they carry a large fraction z_{h} of the photon energy ν (7 GeV $\leq \nu \leq$ 23.4 GeV). How-

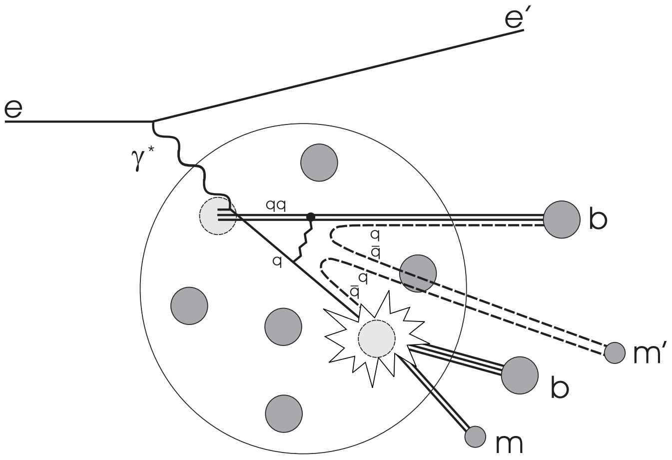

Fig. 1. Illustration of an electron-nucleus interaction: The virtual photon γ^* excites a hadronic string by hitting a quark q inside a bound nucleon. In our example the string between the struck quark q and diquark qq fragments due to the creation of two quark-antiquark pairs. One of the antiquarks combines with the struck quark to form a 'leading' meson m, *one of the created quarks combines with the diquark to form a 'leading' baryon* b. *The remaining partons combine to a meson* m′ *that, depending on the mass of the meson, might leave the nucleus before it hadronizes (see (2)).*

ever, the hadrons with z_h close to 1 (or energy $\approx \nu$) predominantly stem from the string ends and therefore can interact directly after the photon-nucleon interaction. We note, that about 2/3 of the intermediate z_h hadrons (mainly pions) are created from the decay of vector mesons that have been created in the string fragmentation. Because of their higher mass m_h (0.77 − 1.02 GeV), these vector mesons may form (or hadronize) inside the nucleus (see Eq. (2)) and thus suffer from FSI. The effect of the final-state interactions, finally, will depend dominantly on the nuclear geometry, i.e. the size of the target nucleus.

3. Results

3.1. Incoherent ρ^0 production

Incoherent ρ^0 electroproduction off nuclei has been studied in Ref. [4]. In the following, we summarize the results of our investigations. For our model calculations, we demand that the final state has to consist of two oppositely charged pions plus an ensemble of bound nucleons, and we use the kinematic cuts of the HERMES collaboration [22]. This means that we apply the exclusivity measure

$$-2\ \mathrm{GeV} < \Delta E = \frac{p_{\mathrm{Y}}^2 - m_{\mathrm{N}}^2}{2m_{\mathrm{N}}} < 0.6\ \mathrm{GeV}, \tag{8}$$

where m_N denotes the nucleon mass and

$$p_{\mathrm{Y}} = p_{\mathrm{N}} + p_\gamma - p_\rho \tag{9}$$

the 4-momentum of the undetected final state. In Eq. (9), p_γ and p_ρ are the 4-momenta of the incoming photon and the detected $\pi^+\pi^-$ pair and p_{N} is the 4-momentum of the struck nucleon which, for the calculation of p_{Y}, is assumed to be at rest. In addition, we introduce a lower boundary for the four-momentum transfer $|t - t_{\mathrm{max}}| > 0.09\ \mathrm{GeV}^2$ as imposed by the HERMES collaboration to get rid of coherently produced ρ^0.

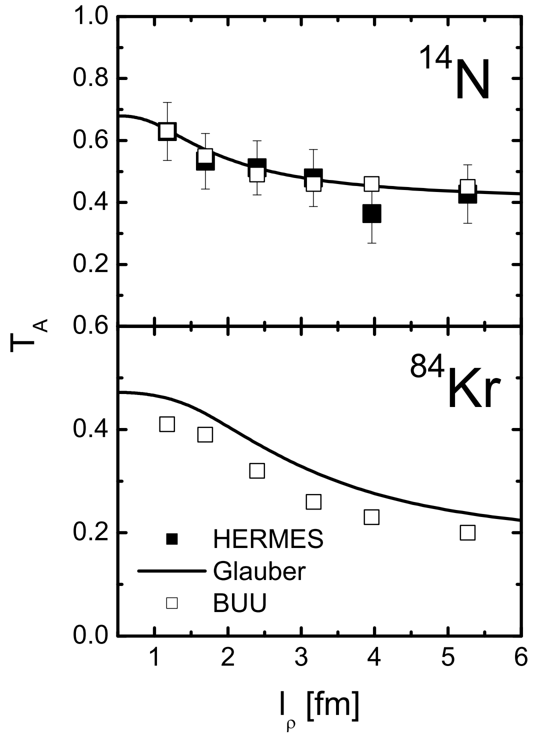

Fig. 2. Nuclear transparency ratio T_{A} for ρ^0 electroproduction plotted versus the coherence length of the ρ^0 component of the photon. The data are taken from [5]. The solid line represents the Glauber result when using Eq. (10). For each transparency ratio calculated within our transport model (open squares), we used the average value of Q^2 and ν of the corresponding data point. The experimental exclusivity measure (8) has been taken into account for both nuclei.

In Fig. 2 we show the transparency ratio T_{A} for exclusive ρ^0 production as a function of the coherence length $l_\rho = q_\rho^{-1}$. The solid line displays the result that one gets if one uses our Glauber expression from Ref. [4]

$$\begin{aligned}\sigma_{\gamma\mathrm{A}\to\rho^0\mathrm{A}^*} &= \sigma_{\gamma\mathrm{N}\to\rho^0\mathrm{N}} \int \mathrm{d}^2 b \int\limits_{-\infty}^{\infty} \mathrm{d}z\, n(\boldsymbol{b}, z) \\ &\times \Bigg| 1 - \int\limits_{-\infty}^{z} \mathrm{d}z_i\, n(\boldsymbol{b}, z_i)(1 - j_0(q_c|z_i - z|)) \frac{\sigma_{\rho\mathrm{N}}}{2} (1 - \mathrm{i}\alpha_\rho) \mathrm{e}^{\mathrm{i}q_\rho(z_i - z)} \\ &\times \exp\left[-\frac{1}{2}\sigma_{\rho\mathrm{N}}(1 - \mathrm{i}\alpha_\rho) \int\limits_{z_i}^{z} \mathrm{d}z_k\, n(\boldsymbol{b}, z_k) \right] \Bigg|^2 \exp\left[-\sigma_\rho^{\mathrm{inel}} \int\limits_{z}^{\infty} \mathrm{d}z'\, n(\boldsymbol{b}, z') \right]. \end{aligned} \tag{10}$$

In Eq. (10) we use for the total ρ^0N cross section $\sigma_{\rho\mathrm{N}} = 25$ mb and for the elastic part $\sigma_\rho^{\mathrm{el}} = 3$ mb. These two values correspond to the ρN cross sections used within the transport model for the involved ρ^0 momenta.

The result of the transport model is represented by the open squares. For each data point we have made a separate calculation with the corresponding values of ν and Q^2. In the case of ^{14}N, the Glauber and the transport calculation are in perfect agreement with each other and the experimental data. This demonstrates that, as we have discussed in Ref. [3], Glauber theory can be used for the FSI if the right kinematic constraints are applied.

After applying all of the above cuts, nearly all of the detected ρ^0 stem from diffractive ρ^0 production for which the formation time is zero. The ^{14}N data seem to support the assumption that the time needed to put the preformed ρ^0 fluctuation on its mass shell and let the wave function evolve to that of a physical ρ^0 is small for the considered values of Q^2. Furthermore, the photon energy is too low to yield a large enough γ factor to make the formation length exceed the internucleon distance and make the colour transparency visible. This conclusion is at variance with that reached in Ref. [6].

We now turn to ^{84}Kr where we expect a stronger effect of the FSI. Unfortunately, there are as yet no data available to compare with. As can be seen from Fig. 2, the transport calculation for ^{84}Kr gives a slightly smaller transparency ratio than the Glauber calculation, especially at low values of the coherence length, i.e. small momenta of the produced ρ^0. There are two reasons for this: About 10% of the difference arises from the fact that within the transport model the ρ^0 is allowed to decay into two pions. The probability that at least one of the pions interacts on its way out of the nucleus is about twice as large as that of the ρ^0. The other reason is that in the Glauber calculation (10) only the inelastic part of the $\rho^0 N$ cross section enters, whereas the transport calculation contains the elastic part as well. Thus all elastic scattering events out of the experimentally imposed t-window are neglected in the Glauber description. It is because of this t-window that also elastic $\rho^0 N$ scattering reduces the transport transparency ratio shown in Fig. 2.

Both effects are more enhanced at lower energies and are negligible for the much smaller ^{14}N nucleus.

3.2. Hadron formation and attenuation in DIS

As mentioned above, hadron production in deep inelastic lepton-nucleus scattering (DIS) offers a way to study the physics of hadronization [23]. The reaction of the exchanged virtual photon (energy ν, virtuality Q^2) with a bound nucleon leads to the production of several hadrons. Depending on the space-time evolution of the production process, the rescattering in the surrounding nuclear medium will change the energy distribution and the multiplicity of the produced particles. Consequently, the particle spectrum of a lepton-nucleus interaction will differ from that of a reaction on a free nucleon. In order to explore such attenuation effects, the HERMES collaboration has investigated the energy ν and fractional energy $z_\mathrm{h} = E_\mathrm{h}/\nu$ dependence of the charged hadron multiplicity ratio

$$R_\mathrm{M}^\mathrm{h}(z_h,\nu) = \left(\frac{N_\mathrm{h}(z_h,\nu)}{N_\mathrm{e}(\nu)}\right)_\mathrm{A} \Bigg/ \left(\frac{N_\mathrm{h}(z_h,\nu)}{N_\mathrm{e}(\nu)}\right)_\mathrm{D} \tag{11}$$

in DIS off N [8] and Kr [9] nuclei. Here $N_\mathrm{h}(z_h,\nu)$ represents the number of semi-inclusive hadrons in a given (z_h,ν)-bin and $N_\mathrm{e}(\nu)$ the number of inclusive DIS leptons in the same ν-bin.

It was suggested in Ref. [8], that a phenomenological description of the R_M^h data can be achieved if the formation time, i.e. the time that elapses from the moment when the photon strikes the nucleon until the reaction products have evolved to physical hadrons, is assumed to be proportional to $(1 - z_\mathrm{h})\nu$ in the target rest frame. This $(1 - z_\mathrm{h})\nu$ dependence of the formation time τ_f is compatible with the gluon-bremsstrahlung model of Ref. [24]. In the investigations of Ref. [8], any interaction of the reaction products with the remaining nucleus during this formation time has been neglected. After the formation time, the hadrons could get absorbed according to their full hadronic cross section. Another interpretation of the observed R_M^h spectra – as being due to a combined effect of a rescaling of the quark fragmentation function in nuclei due to partial deconfinement as well as the absorption of the produced hadrons – has recently been given by the authors of Ref. [13]. Furthermore, calculations based on a pQCD parton model [14, 15] explain the attenuation observed in the multiplicity ratio solely by partonic multiple scattering and induced gluon radiation. It has already been pointed out by the authors of Ref. [13] that a shortcoming of the existing models is the purely absorptive treatment of the final-state interactions (FSI). We avoid this problem by using the coupled-channel transport model.

In our calculation, we employ the kinematic cuts of the HERMES experiment as well as the geometrical cuts of the detector. In actual numbers: we require for the Bjorken scaling variable $x = Q^2/(2m_\mathrm{N}\nu) > 0.06$ (with m_N denoting the nucleon mass), for the photon virtuality $Q^2 > 1$ GeV^2 and for the energy fraction of the virtual photon $y = \nu/E_\mathrm{beam} < 0.85$. In addition, the PYTHIA model introduces a lower cut in the invariant mass of the photon-nucleon system at $W = 4$ GeV that is above the experimental constraint $W > 2$ GeV. This limits our calculations to the minimal photon energies of $\nu_{\min} = 8.6$ GeV as compared to $\nu_{\min} = 7$ GeV in the HERMES experiment and leads to a suppression of high Q^2 events at energies below $\nu \approx 15$ GeV.

We have shown in Ref. [7] that our model simulation reproduces the experimental average values of the kinematic variables Q^2 and ν (z_h) on N and Kr as a function of z_h (ν) very well. Since the particles with z_h close to 1 are predominantly leading hadrons, we could use the high z_h part in the fractional energy spectrum to fix the leading hadron cross section. A good agreement with the data is achieved for $\sigma_\mathrm{lead} = 0.33\sigma_\mathrm{h}$ during the formation time τ_f. We note, that this value for σ_lead represents an average value over time from the virtual photon-nucleon interaction to the actual hadron formation time. Since for light nuclei only a fraction of the

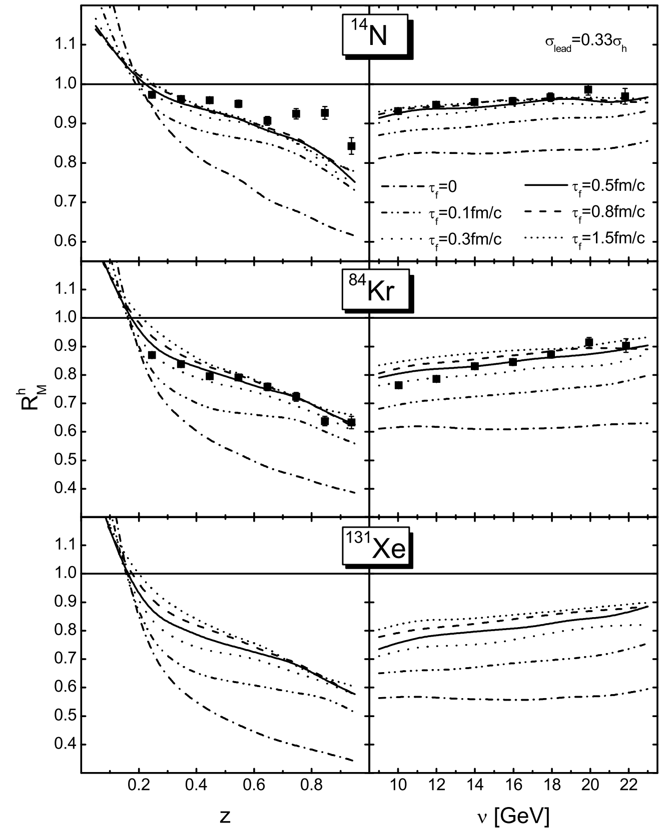

Fig. 3. Calculated multiplicity ratios of charged hadrons for N, Kr *and* Xe *targets for a fixed leading hadron cross section $\sigma_\mathrm{lead} = 0.33\sigma_\mathrm{h}$ and different values of the formation time τ_f. The data for the nitrogen target have been taken from Ref. [8], while the preliminary* Kr *data stem from Ref. [9].*

leading hadrons is formed inside the nucleus, the effective leading hadron cross section σ_{lead} is expected to be smaller accordingly. For a detailed investigation we refer the reader to a forthcoming study [25].

In Fig. 3 we show the influence of different formation times τ_{f} on $R_{\mathrm{M}}^{\mathrm{h}}$ using the effective cross section $\sigma_{\mathrm{lead}} = 0.33\sigma_{\mathrm{h}}$. We find, that formation times $\tau_{\mathrm{f}} \gtrsim 0.3$ fm/c are needed to describe the experimental data with little sensitivity to higher values. This is compatible to the range of values extracted from the antiproton attenuation studies in Ref. [26].

Some of our model assumptions, e.g. the local density approximation, become questionable for very light nuclei. We have, therefore, used the Kr data to fix the value of the formation time. However, we also get a satisfying agreement with the nitrogen data.

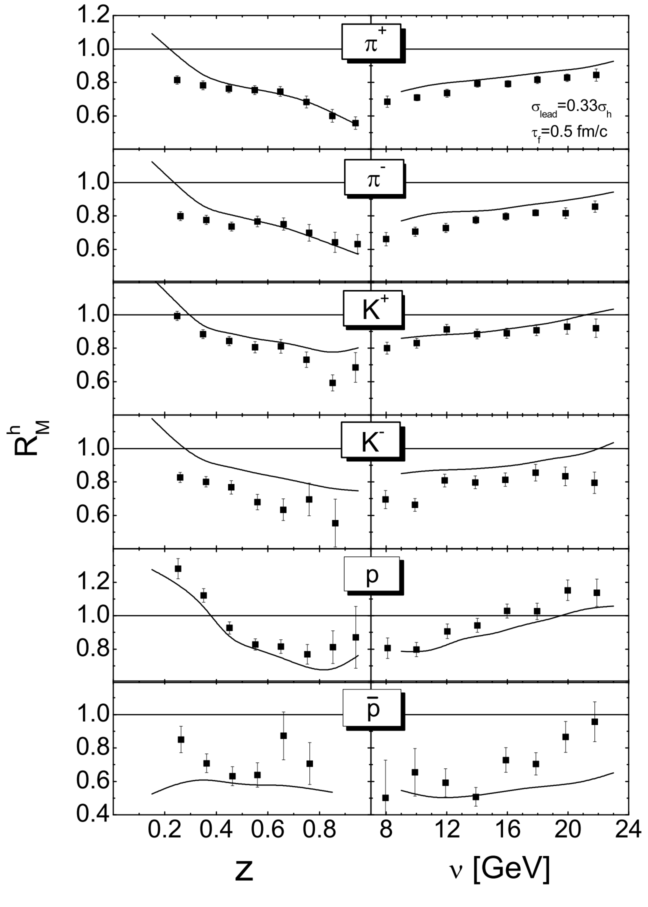

Fig. 4. Calculated multiplicity ratios of π^+, π^-, K^+, K^-, p and $\bar{\mathrm{p}}$ for krypton using a fixed leading hadron cross section $\sigma_{\mathrm{lead}} = 0.33\sigma_{\mathrm{h}}$ and formation time $\tau_{\mathrm{f}} = 0.5$ fm/c. The experimental data has been taken from Ref. [27].

The pQCD model of Ref. [14] predicts a hadron attenuation $\sim A^{2/3}$ since the parton energy loss is proportional to the propagation length squared. It is thus important to get the scaling with target mass A from our present approach in order to allow experimental studies to distinguish between the different concepts. To this aim, Fig. 3 also shows predictions for a Xe target. In accordance with the authors of Ref. [13], we predict only a small change in the multiplicity spectra compared to the Kr target such that the scaling exponent is lower than 2/3.

In Fig. 4 we show the results for the calculated multiplicity ratio of π^-, π^+, K^-, K^+, p and $\bar{\mathrm{p}}$ for Kr in comparison with the experimental data. In our calculations we use again the kinematic cuts of the HERMES experiment with the additional restrictions $x \geq 0.02$, $E_{\pi,\mathrm{K}}$=2.5 − 15 GeV and $E_{\mathrm{p},\bar{\mathrm{p}}} = 4-15$ GeV that are experimentally necessary for particle identification [27]. We use a constant formation time of 0.5 fm/c and $\sigma_{\mathrm{lead}} = 0.33\sigma_{\mathrm{h}}$ for all hadrons. Without further fine tuning, we get a satisfying description of all the data meaning that the formation times of mesons, baryons and antibaryons are about equal.

4. *Summary*

We have developed a method to account for coherence length effects within a semi-classical BUU transport model. This allows us to describe incoherent meson photo- and electroproduction off nuclei at GeV energies using a full coupled-channel treatment of the FSI. We have calculated the transparency ratio for exclusive incoherent ρ^0 photoproduction off ^{14}N and ^{84}Kr. The result for ^{14}N is in agreement with experimental data and with the Glauber prediction. The latter shows that in the case of ^{14}N, Glauber theory is applicable after the kinematic cuts of the HERMES experiment are applied. Since we do not use a formation time for diffractively produced vector mesons, we deduce that one cannot see an onset of colour transparency in the nitrogen data. For the ^{84}Kr target, no experimental data is available to compare with. However, we find deviations from the simple Glauber model because of the finite life time of the ρ^0 and elastic scattering out of the kinematically allowed $|t|$-region. As discussed by Kopeliovich et al. [6], one might see an onset of colour transparency when investigating the transparency ratio as a function of Q^2 for fixed coherence length.

In addition, we have shown that one can describe the experimental data of the HERMES collaboration for hadron attenuation on nuclei without invoking any changes in the fragmentation function due to gluon radiation. In our dynamical studies, that include the most relevant FSI, we employ only the 'free' fragmentation function on a nucleon and attribute the hadron attenuation to the deceleration of the produced hadrons due to FSI in the surrounding medium. We find that in particular the z-dependence of $R_{\mathrm{M}}^{\mathrm{h}}$ is very sensitive to the interaction cross section of leading hadrons and can be used to determine σ_{lead}. The interaction of the leading hadrons during the formation time could be interpreted as an in-medium change of the fragmentation function. The extracted average hadron formation times of

$\tau_\mathrm{f} \gtrsim 0.3$ fm/c are compatible with the analysis of antiproton attenuation in $\mathrm{p}+\mathrm{A}$ reactions at AGS energies [26].

In this work, we have also for the first time compared our results for the attenuation of π^-, π^+, K^-, K^+, p and $\bar{\mathrm{p}}$ with the Kr experimental data. We find a satisfying description of all data using the same constant formation time τ_f=0.5 fm/c and the same reduction of the effective leading hadron cross section σ_lead=0.33 fm/c for all hadron species.

Acknowledgements

This paper is based on work done together with W. Cassing and K. Gallmeister. The authors acknowledge valuable discussions with A. Borissov, C. Greiner and V. Muccifora. This work was supported by DFG and BMBF.

References

[1] A. H. Mueller, in *Proc. 17th Recontre de Moriond, Moriond, 1982*, ed. J. Tran Tanh Van, Editions Frontieres, Gif-sur-Yvette Cedex, France (1982) p. 13; S. J. Brodsky, in *Proc. 13th Symp. Multiparticle Dynamics*, eds. W. Kittel, W. Metzger and A. Stergiou, World Scientific, Singapore (1982).

[2] M. Effenberger and U. Mosel, Phys. Rev. C **62** (2000) 014605.

[3] T. Falter and U. Mosel, nucl-th/0202011; T. Falter and U. Mosel, Phys. Rev. C **66** (2002) 024608.

[4] T. Falter, K. Gallmeister and U. Mosel, Phys. Rev. C **67** (2003) 054606.

[5] A. Airapetian et al., HERMES Collaboration, Phys. Rev. Lett. **90** (2003) 052501.

[6] B. Z. Kopeliovich, J. Nemchik, A. Schaefer and A. V. Tarasov, Phys. Rev. C **65** (2001) 035201.

[7] T. Falter, W. Cassing, K. Gallmeister and U. Mosel, Phys. Lett. B **594** (2004) 61.

[8] A. Airapetian et al., HERMES Collaboration, Eur. Phys. J. C **20** (2001) 479.

[9] V. Muccifora, HERMES Collaboration, Nucl. Phys. A **711** (2002) 254; E. Garutti, HERMES Collaboration, Act. Phys. Pol. B **33** (2002) 3013.

[10] S. A. Bass et al., Prog. Part. Nucl. Phys. **41** (1998) 225.

[11] J. Geiss, W. Cassing and C. Greiner, Nucl. Phys. A **644** (1998) 107.

[12] W. Cassing and E. L. Bratkovskaya, Phys. Rep. **308** (1999) 65.

[13] A. Accardi, V. Muccifora and H. J. Pirner, Nucl. Phys. A **720** (2003) 131.

[14] X. Guo and X. N. Wang, Phys. Rev. Lett. **85** (2000) 3591; X. N. Wang and X. Guo, Nucl. Phys. A **696** (2001) 788; E. Wang and X. N. Wang, Phys. Rev. Lett **89** (2002) 162301; X. N. Wang, Nucl. Phys. A **715** (2003) 775.

[15] F. Arleo, Eur. Phys. J. C 30 (2003) 213.

[16] K. Gallmeister, C. Greiner and Z. Xu, Phys. Rev. C **67** (2003) 044905.

[17] T. Sjostrand, P. Eden, C. Friberg, L. Lonnblad, G. Miu, S. Mrenna and E. Norrbin, Comput. Phys. Commun. **135** (2001) 238; T. Sjostrand, L. Lonnblad and S. Mrenna, hep-ph/0108264.

[18] C. Friberg and T. Sjostrand, J. HEP **0009**, 010 (2000).

[19] T. Falter, S. Leupold and U. Mosel, Phys. Rev. C **62** (2000) 031602(R).

[20] M. Effenberger, E. L. Bratkovskaya and U. Mosel, Phys. Rev. C **60** (1999) 044614.

[21] K. Hagiwara et al., *Review of Particle Physics*, Phys. Rev. D **66** (2002) 010001.

[22] K. Ackerstaff et al., Phys. Rev. Lett. **82** (1999) 3025.

[23] B. Kopeliovich, J. Nemchik and E. Predazzi, hep-ph/9511214.

[24] B. Kopeliovich, J. Nemchik and E. Predazzi, Proc. Workshop on Future Physics at HERA, eds. G. Ingelman, A. De Roeck and R. Klanner, DESY (1995/1996) vol. 2, 1038 (nucl-th/9607036).

[25] T. Falter, W. Cassing, K. Gallmeister and U. Mosel, nucl-th/0406023.

[26] W. Cassing, E. L. Bratkovskaya and O. Hansen, Nucl. Phys. A **707** (2002) 224.

[27] A. Airapetian et al., HERMES Collaboration, Phys. Lett. B **577** (2003) 37.

ELEKTROTVORBA HADRONA U JEZGRAMA NA GeVSKIM ENERGIJAMA

Istražujemo učinke duljine koherencije i slabljenja hadrona u raspršenju leptona u jezgrama u kinematskin uvjetima mjerenja HERMES. Osnovno se međudjelovanje elektrona s nukleonom opisuje pomoću generatora događaja PYTHIA, dok je potpun opis međudjelovanja u konačnom stanju vezanim kanalima uključen transportnim modelom BUU. Ishodi naših računa su u dobrom skladu s mjerenim omjerom propusnosti nekoherentne elektrotvorbe ρ^0 u ^{14}N i omjera višestrukosti $R_{\mathrm{M}}^{\mathrm{h}}$ za nabijene hadrone, pione, protone i antiprotone u duboko neelastičnom raspršenju u metama ^{14}N i ^{84}Kr.